

# Enhancement in the Electrical and Thermal Properties of Ethylene Vinyl Acetate (EVA) Co-Polymer by Zinc Oxide Nanoparticles

Jose Sebastian<sup>1</sup>, Eby T. Thachil<sup>1</sup>, Jobin Job Mathen<sup>2</sup>, Joseph Madhavan<sup>2</sup>, Prince Thomas<sup>3</sup>, Jacob Philip<sup>4</sup>, M. S. Jayalakshmy<sup>4</sup>, Shahrom Mahmud<sup>5</sup>, Ginson P. Joseph<sup>3\*</sup>

<sup>1</sup>Department of Polymer Science and Rubber Technology, Cochin University of Science and Technology, Kerala, India

<sup>2</sup>Department of Physics, Loyola College, Chennai, India

<sup>3</sup>Department of Physics, St. Thomas College, Palai, India

<sup>4</sup>Department of Instrumentation, Cochin University of Science and Technology, Kerala, India

<sup>5</sup>School of Physics, Universiti Sains Malaysia, Minden, Malaysia

Email: [joseuce@gmail.com](mailto:joseuce@gmail.com), [etthachil@gmail.com](mailto:etthachil@gmail.com), [jobinjobuv@gmail.com](mailto:jobinjobuv@gmail.com), [jmadhvang@yahoo.com](mailto:jmadhvang@yahoo.com), [princealani@gmail.com](mailto:princealani@gmail.com), [jphilip6012@gmail.com](mailto:jphilip6012@gmail.com), [jayalakshmy.ms@gmail.com](mailto:jayalakshmy.ms@gmail.com), [ginsonpj@gmail.com](mailto:ginsonpj@gmail.com), [ginsonpjoseph@gmail.com](mailto:ginsonpjoseph@gmail.com)

Received 21 May 2015; accepted 4 July 2015; published 7 July 2015

Copyright © 2015 by authors and Scientific Research Publishing Inc.

This work is licensed under the Creative Commons Attribution International License (CC BY).

<http://creativecommons.org/licenses/by/4.0/>



Open Access

## Abstract

EVA/ZnO nanocomposites of 1%, 2% and 4% ZnO were fabricated by direct probe sonicator method. The ZnO nanopowders were prepared by solvothermal method. As the particle size of the filler incorporated to the polymer matrix decreases, the properties of the polymer-filler interface show dominance over its bulk properties. The dielectric constant and dielectric loss of the composites at ambient temperatures are found to decrease with increasing frequency. The thermal analysis using TGA-DTA is also performed and it is found that the thermal stability of the nanocomposites increases with increasing the filler concentrations. The thermal parameters such as thermal diffusivity ( $\alpha$ ) and thermal effusivity ( $e$ ), the thermal conductivity ( $k$ ) and heat capacity ( $C_p$ ) were studied using photopyroelectric technique. The band gap of the samples was also determined and found to decrease with increasing filler concentrations. The tensile strength and peel strength of the samples were also investigated and it is found to increase with small inclusion of filler material.

## Keywords

Composite Materials, Polymers, Differential Thermal Analysis (DTA), Dielectric Properties

\*Corresponding author.

## 1. Introduction

Composites have attracted attention of material scientists as it can combine advantages of different materials. In recent years, material scientists are looking for nano-composites based on polymer matrix due to several added advantages. The advantages include balanced physical and mechanical properties, ease of processability and low production cost [1]. Many previous works have been carried out to improve the optical and electrical properties of polymers through suitable doping [2] [3]. Polymer based dielectric materials can give flexible and light weight electrical devices. It is discovered that nano-particles like  $\text{Al}_2\text{O}_3$ ,  $\text{TiO}_2$ ,  $\text{SiO}_2$  etc. heterogeneously distributed within the polymer matrix can enhance dielectric properties [4]. Murugaraj and co-workers [5] have fabricated polymer-alumina nano-composites with improved dielectric characteristics. Carbon nanotubes (CNTs), carbon black, carbon nanofibres (CNF) as well as single and multi wall carbon nano tubes (SWNTs & MWNTs) have been incorporated to polymer matrix to use as antistatic coatings [6].

During recent years, colloidal and semiconducting nano particles have attracted a great deal of attention for both researchers and industrialists. Different types of group II-VI nano particles including ZnSe, CdS, CdSe, CdTe are found to be used extensively for light-emitting diode [7], solar cell [8], biomedical tag [9] and laser [10] applications. Nanocrystals (NCs) of semi conducting materials are used in optoelectronic devices like lasers and transistors [11] [12]. The ZnO used in this study is one such type of nanopowder having excellent ultraviolet and visible photoluminescence [13], and it is a semiconductor having large exciton binding energy (60 meV). It has got diverse applications in photovoltaic cells, variable resistors, as fully transparent thin film transistors and in short wavelength light emitting diodes.

Wide variety of polymers are found application in the synthesis of nano composites. They form the continuous phase termed as the matrix of the composite. Polymer matrix composites (PMC) with ceramic and metals as fillers have been developed to improve electrical properties like dielectric permittivity [14] [15]. Poly methylmethacrylate [16] [17], epoxy [18], poly(vinyl alcohol) [19], polyaniline [20] [21] are extensively used as the matrix for composites.

Poly (ethylene-co-vinyl acetate), EVA, was used as the base polymer in this experiment as they are compatible even with inert fillers. EVA is noted for its rubbery nature along with gloss, permeability and good impact strength. EVA- $\text{TiO}_2$  nanocomposites were investigated for the effect of  $\text{TiO}_2$  particle size on the co-efficient of thermal expansion [22]. EVA copolymer irradiated with gamma rays can cause modification in its electronic structure [23]. Ethylene vinyl acetate is particularly used in electrical industry as cable insulating material due to good stress cracking resistance.

The II-VI semiconducting materials show significant properties from the optoelectronic point of view [24]. In the bulk form and in the quantum dot form these materials exhibit high density and quantum confinement. This paper deals with the effect of ZnO nanopowder on the electrical, optical, mechanical properties EVA polymer matrix and reported for the first time.

## 2. Synthesis of ZnO Nanoparticle

A solution of 0.2M- $(\text{CH}_3\text{COO})_2\text{Zn}\cdot 2\text{H}_2\text{O}$ , Zinc Acetate, was prepared by dissolving 4.39 gm of  $(\text{CH}_3\text{COO})_2\text{Zn}\cdot 2\text{H}_2\text{O}$  in 100 ml of methanol in a beaker and the mixture was kept stirred for 15 minutes. Another mixture of 0.5M-NaOH and methanol was prepared by dissolving 0.5 gm of NaOH in 25 ml of methanol and was kept for stirring for 15 minutes. Then the NaOH-methanol mixture was added to the basic solution and the reaction mixture was kept stirred for 30 minutes. The prepared solution was kept in autoclave for drying at  $180^\circ\text{C}$  for 5 hours to obtain nano-sized ZnO particles. Dried ZnO nanoparticles, white in colour was obtained. The size of the nanopowder was determined using TEM and it as confirmed 20 nm (Figure 1).

### Synthesis of ZnO/EVA Polymer Nanocomposite

Poly (ethylene-co-vinyl acetate), EVA copolymer used for the experiment was obtained from ExxonMobil Chemicals, Singapore. The vinyl acetate content of the copolymer used was 9.4 wt% (Density— $0.931\text{ g/cm}^3$ , Melt Flow Index— $2.1\text{ g/10min @}190^\circ\text{C}$ , 2.16 kg). Ethylene Vinyl Acetate-ZnO nanocomposites were prepared for different weight percentage (1%, 2%, and 4%) of ZnO by direct probe sonicator method. Initially pure EVA film was made in a glass mould by solvent casting method using toluene. Then 1% by weight of ZnO nanoparticles was added to EVA- toluene mixture taken in a beaker and was subjected to direct probe sonication. Finally

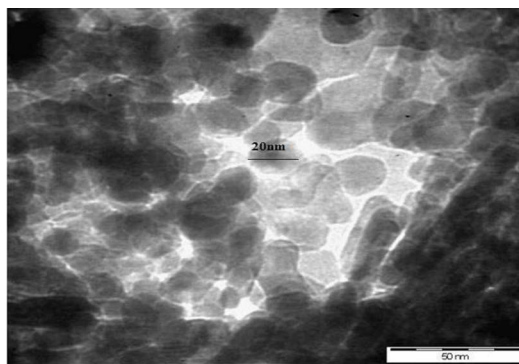


**Figure 1.** TEM image of ZnO nanopowder.

the polymer was dried in a glass mould for 3 - 4 hours at 50°C and thus polymer nanocomposite with 1% ZnO was formed. Similarly nanocomposites for remaining weight percentage, (2% and 4%) of ZnO were prepared.

### 3. Results and Discussion

#### 3.1. Morphological Studies

TEM micrograph shown in **Figure 1** confirmed that the synthesized ZnO powder are solid in nature and obtained particle size is about 20 nm. SEM micrographs were used to identify the relative differences in surface characteristics of EVA and its nanocomposites. The ZnO particle distribution and its influence on the EVA copolymer morphology were also investigated. The interaction between ZnO with host matrix is strong and the surface micelles are homogeneous. Micrographs at 10  $\mu\text{m}$  and 1  $\mu\text{m}$  showed the developed shape of the EVA particles and the filler distribution in EVA as shown in **Figure 2(b)** & **Figure 2(c)**. A homogeneous dispersion of ZnO in the EVA matrix was observed in **Figure 2(a)**. The nano ZnO dispersion in the EVA surface was evident with higher magnification at 100 nm.

#### 3.2. Electrical and Optical Properties

The ZnO/EVA polymer nanocomposite of area 15 mm<sup>2</sup> having silver coating on the opposite faces was introduced between two copper electrodes and then connected to HIOKI 3532-50 LCR Impedance analyzer for dielectric measurement. The dielectric constant of the sample is calculated using the relation  $\epsilon = Cd/\epsilon_0 A$ ; where the nanocomposite acts as a dielectric with  $\epsilon_0$  the absolute permittivity, C is the capacitance, d is the thickness and A is the area (mm<sup>2</sup>) of the ZnO/EVA composite. **Figure 3** shows the variation of dielectric constant of ZnO/EVA with different filler concentrations. From the figure one can easily examine the behaviour of dielectric constant of nanocomposites with varying frequency from 100 Hz to 5 MHz. It is observed that initially the dielectric constant has larger values at lower frequencies and then decreases with increase in frequency for all films; however there is an increase in the dielectric constant of the nanocomposites as the percentage of the filler concentrations increases. The value of dielectric constant at 1 KHz for 1%, 2% and 4% are around 3.62, 4.1 and 4.87 respectively. The dielectric constant remains almost constant for all samples in the higher frequencies. At low frequencies, all the four polarizations are active. The space charge contribution depends on the purity and perfection of the material and its influence is noticeable in the low frequency region. The orientational effect can sometimes be seen in some materials even up to 10<sup>10</sup> Hz. Ionic and electronic polarizations always exist below 10<sup>13</sup> Hz. Hence, the larger values of dielectric constant and dielectric loss exhibited by nanocomposite at low frequencies may be attributed to space charge polarization due to impurities and defects present in the nanocomposites. **Figure 4** shows the variation of dielectric loss of nanocomposites as a function of frequency. In the lower frequency region, dielectric loss shows larger values due to the loss associated with ionic mobility. The trend in the variations of both dielectric constant and dielectric loss as a function of frequency is the same. Temperature has a striking effect on the dielectric properties. Interestingly, the variations of both dielectric constant and dielectric loss as a function of frequency are the same for all temperatures. It is observed that the dielectric constant and dielectric loss slightly decrease with the temperature which may due to the reduction in charge carriers. The variation of dielectric constant and loss with temperatures for 1 KHz and 2 KHz frequency

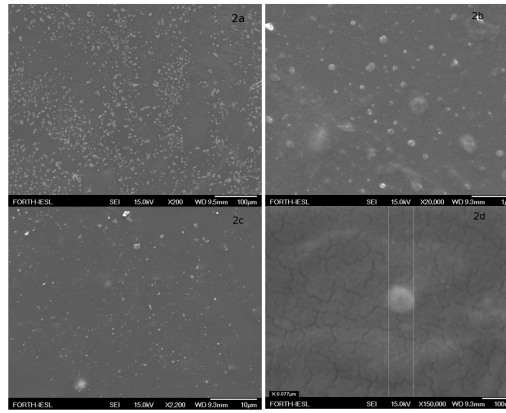


**Figure 2.** (a)-(d) SEM Micrographs of ZnO/EVA nanocomposite in different magnifications.

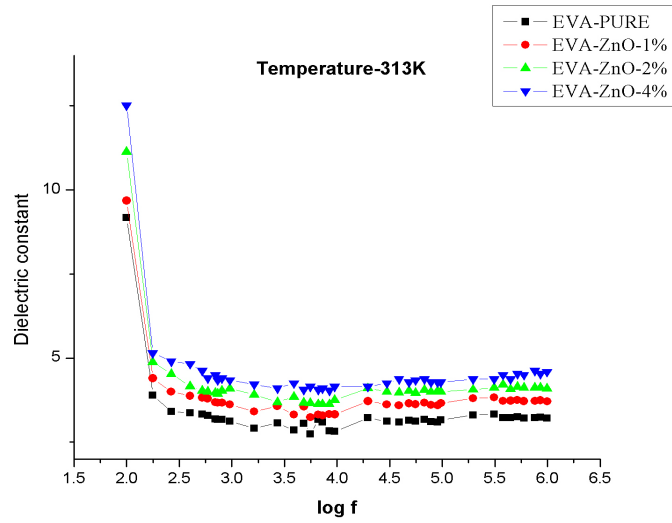


**Figure 3.** Variation of dielectric constant of ZnO/EVA with different filler concentrations as a function of frequency.

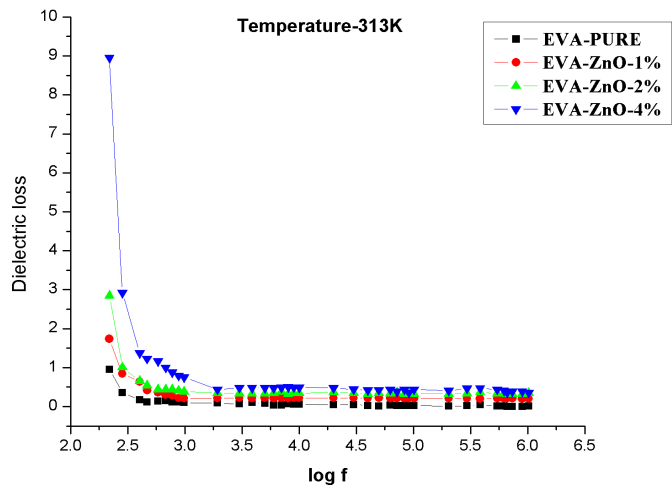


**Figure 4.** Variation of dielectric loss of ZnO/EVA with different filler concentrations as a function of frequency.

are shown in **Figures 5-8**.

The optical absorption coefficients of the nanocomposites are done using VARIAN CARY 5000 spectrophotometer in the range of 200 to 2000 nm and are shown in **Figure 9**. The spectra show large transparency window between 500 nm and 1600 nm. But there is a absorption at 1200 and 1450 nm. It is observed that the intensity of the absorption peak is increased with increasing the filler concentrations. The band gap of the PNC's are calculated using Tauc plotting technique and is shown in **Figure 10**. The band gaps of 1%, 2% and 4% EVA/ZnO PNC's are found to be 4.56 eV, 4.18 eV and 3.97 eV respectively, which decreases with increasing filler concentrations thus increases the conductivity by increasing the ZnO concentration.

The analysis of Fourier transform infrared (FT-IR) spectra of the samples have been carried out using a Thermo Nicolet Make Avatar 370 FTIR Spectrometer in the wave number range 400 - 4000  $\text{cm}^{-1}$ . DTGS detector is used for signal Detection. **Figures 11(a)-(c)** show the FT-IR spectra of pristine EVA and 2% & 4% ZnO/EVA nanocomposites. The spectrum of the nanocomposites exhibits the characteristics absorption bands

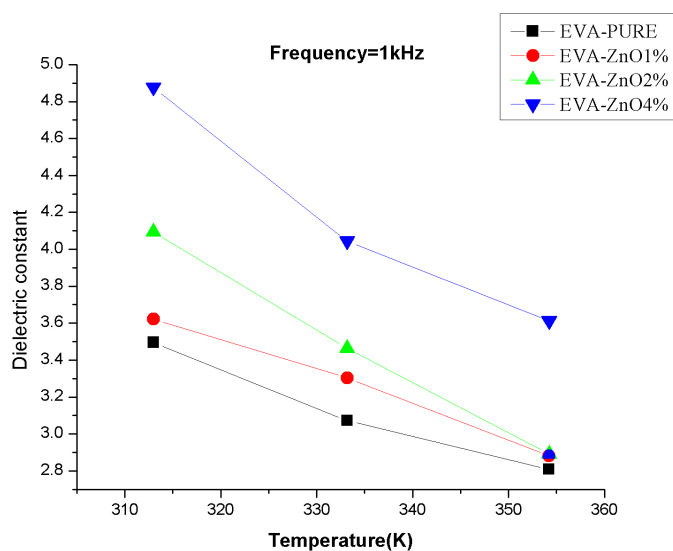


**Figure 5.** Variation of dielectric constant of ZnO/EVA with different temperature at 1 KHz frequency.

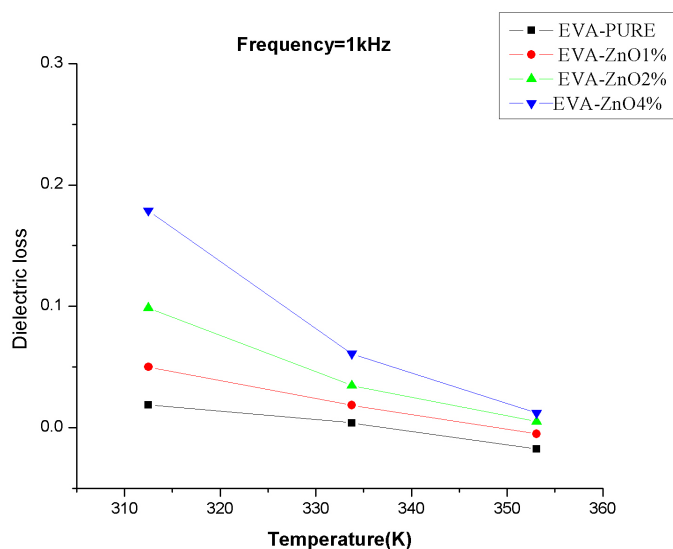


**Figure 6.** Variation of dielectric loss of ZnO/EVA with different temperature at 1 KHz frequency.

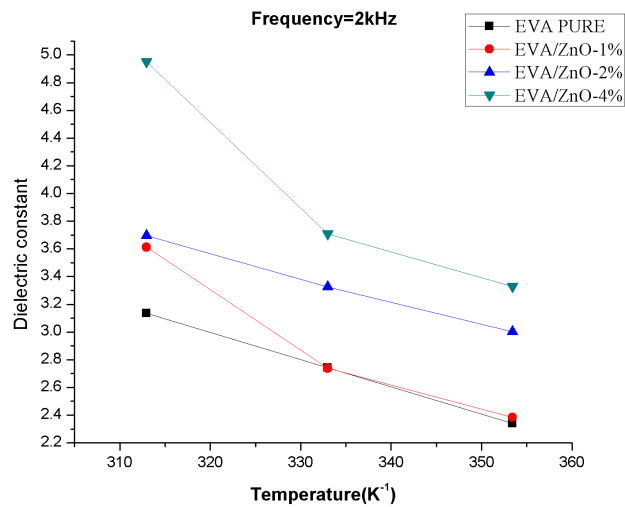


**Figure 7.** Variation of dielectric constant of ZnO/EVA with different temperature at 2 KHz frequency.

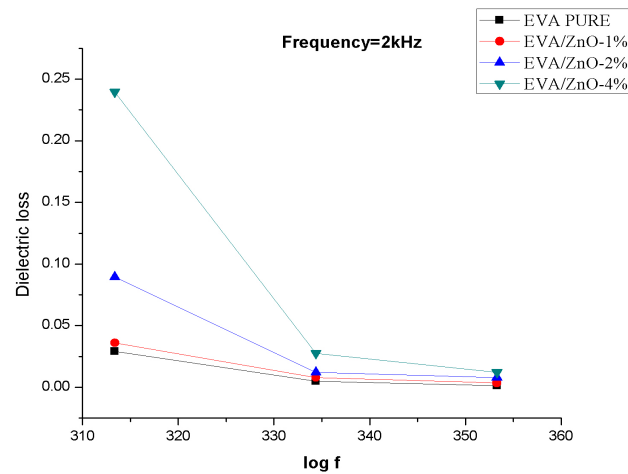


**Figure 8.** Variation of dielectric loss of ZnO/EVA with different temperature at 2 KHz frequency.

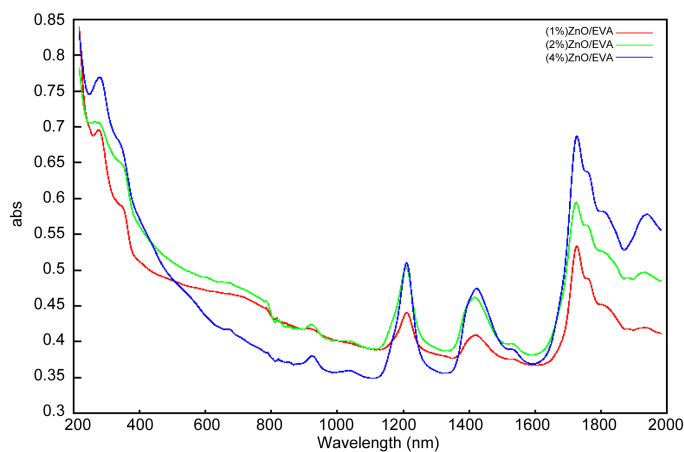


**Figure 9.** UV-Vis-NIR spectra of EVA/ZnO Nanocomposite with different filler concentrations.

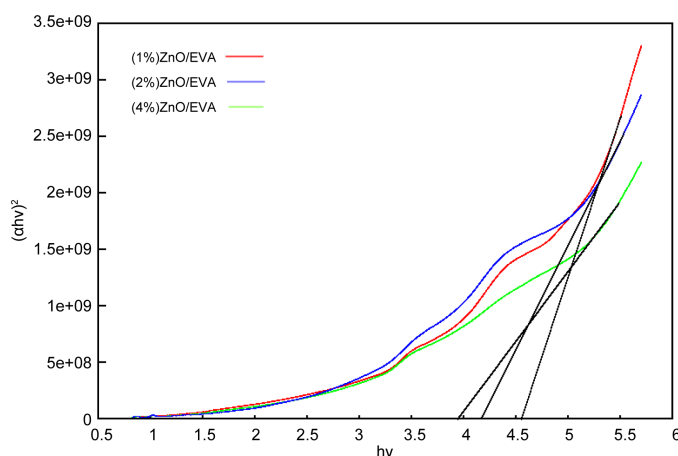


**Figure 10.** Tauc plot of EVA/ZnO nanocomposite with different filler concentrations.

corresponding to polymer groups and ZnO nanoparticles. In following spectra of ZnO/EVA composites, the transmittance intensity changes at  $479.24\text{ cm}^{-1}$ ,  $444.73\text{ cm}^{-1}$  and  $434\text{ cm}^{-1}$  are corresponding to Zn-O vibrations. The bands centered at  $1371.96\text{ cm}^{-1}$  and  $1163.75\text{ cm}^{-1}$  are indicates the transmittance intensity is increased and is attributed to the stretching vibrations of C=O and C-H groups in acetate species.

The characteristics vibration bands of aromatic C=C units are observed at  $1465.70\text{ cm}^{-1}$  in the spectra of EVA and ZnO/EVA has changed as increasing percentages of ZnO nanoparticles and extra peaks are observed at  $1566.25\text{ cm}^{-1}$  and  $1624.13\text{ cm}^{-1}$ . The band centered at  $2920\text{ cm}^{-1}$  and  $2850.28\text{ cm}^{-1}$  are observed in EVA and ZnO/EVA spectra are the stretching vibrations of C-H alkanes. There is a specific peak is observed in the spectrum of both 2% and 4% ZnO/EVA at  $3431.14\text{ cm}^{-1}$  and  $3396.19\text{ cm}^{-1}$  which emphasized the O-H bond stretching of ZnO nanofillers. The changes in the relative intensities of the bands in the region  $1420.31\text{ cm}^{-1}$ ,  $1115\text{ cm}^{-1}$  and  $902.61\text{ cm}^{-1}$  in composite can be due to the presence of absorbed species on the surface of the ZnO nanoparticles. The characteristics bands of EVA and ZnO are both observed in the ZnO/EVA spectrum which confirmed that ZnO is well dispersed in the EVA matrix.

### 3.3. Thermal Studies

The TGA and DTA analyses of polymer nanocomposites were carried out between  $28^\circ\text{C}$  and  $1300^\circ\text{C}$  at a heating rate of  $20\text{ K/min}$  using the instrument NETSZCH STA 409C. The TGA-DTA curves are shown in **Figures 12(a)-(d)**, which confirms the decomposition of the nanocomposites occurs in two steps.  $28.9\%$  and  $28.5\%$  of weight is lost for Pure EVA and 1% added composite respectively in the first stage while that of  $14\%$  and  $13\%$  respectively for 2% and 4% of filler concentrations. It is also observed that the thermal stability of the polymer nanocomposites increases with increasing the filler concentrations and the onset decomposition temperature of the pure EVA, 1%, 2% and 4% are around  $290^\circ\text{C}$ ,  $295^\circ\text{C}$ ,  $318^\circ\text{C}$  and  $337^\circ\text{C}$  respectively. There is no much difference in the thermogram of Pure and 1% doped ZnO. The increment in the thermal stability may be due to the increase in the strength of the nanocomposite by increase of interfacial area.

The thermal parameters such as thermal diffusivity ( $\alpha$ ) and thermal effusivity ( $e$ ), the thermal conductivity ( $k$ ) and heat capacity ( $C_p$ ) were determined by the technique developed Preethy C menon *et al.* [25]. During the measurement the sample, the pyroelectric detector and the backing should be thermally thick. The sample was illuminated by an intensity-modulated beam of light, which gives rise to periodic temperature variation by optical absorption. The thermal waves so generated propagate through the sample and were detected by the pyroelectric detector.

A He-Cd laser of (wavelength  $\lambda = 442\text{ nm}$  KIMMON) output power  $120\text{ mW}$  was used as the optical heating source. A polyvinylidene difluoride (PVDF) film of thickness  $28\text{ }\mu\text{m}$  was used as the pyroelectric detector. The sample was attached to the pyroelectric detector by means of a thermally thin layer of a compound whose contribution to the signal was negligible. The signal output was measured using a lock-in amplifier (SR830). The frequency of modulation of the light was kept above  $40\text{ Hz}$  to ensure that the detector, the sample and the backing

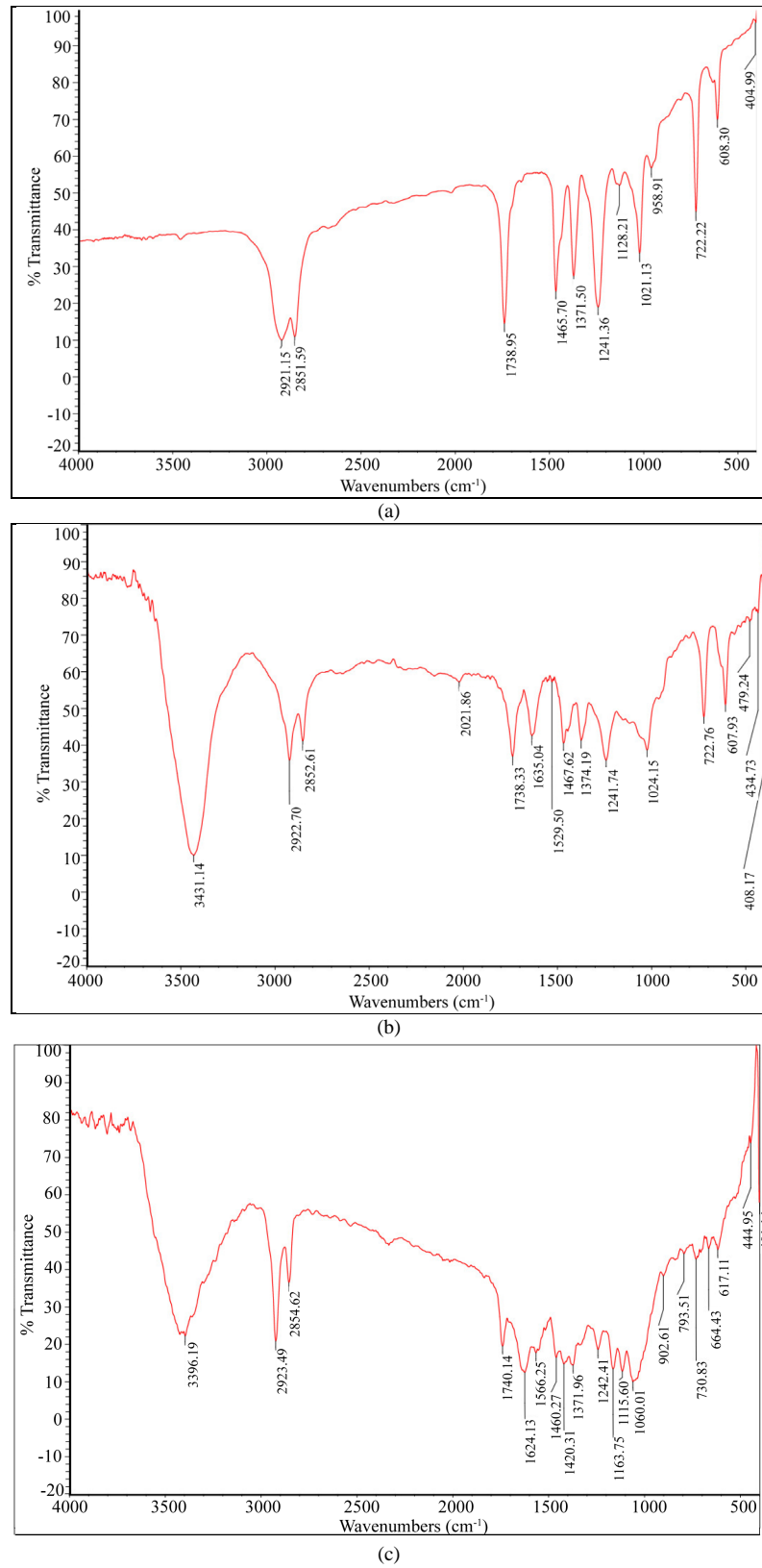
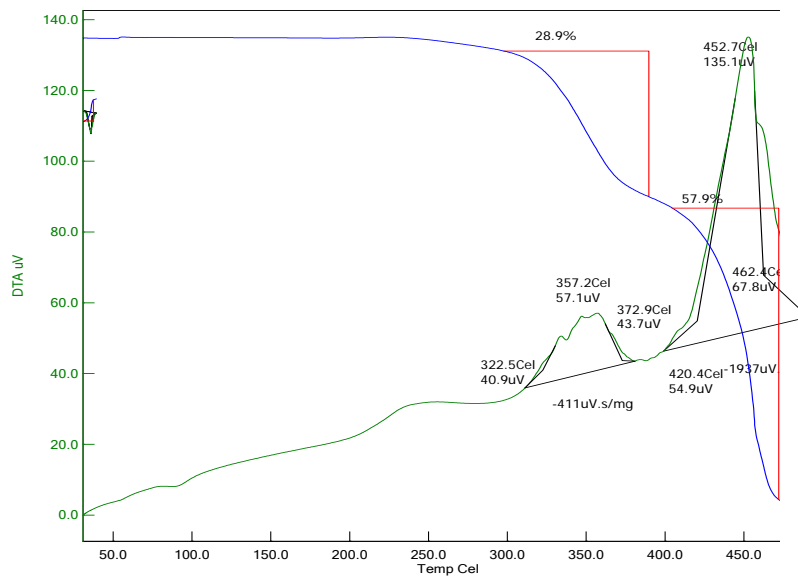
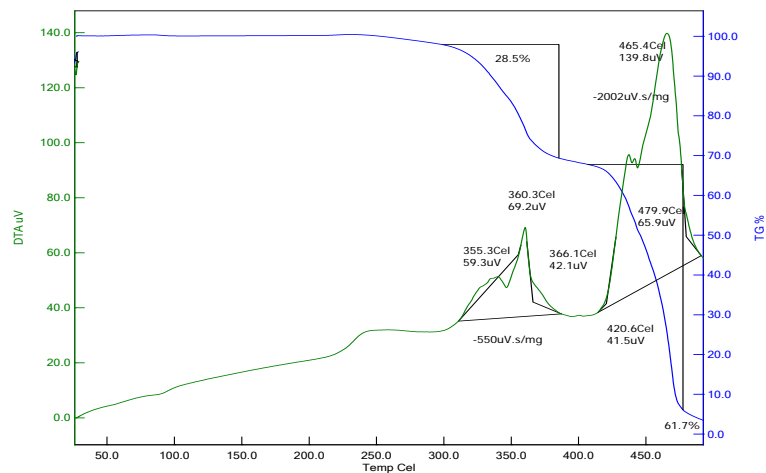


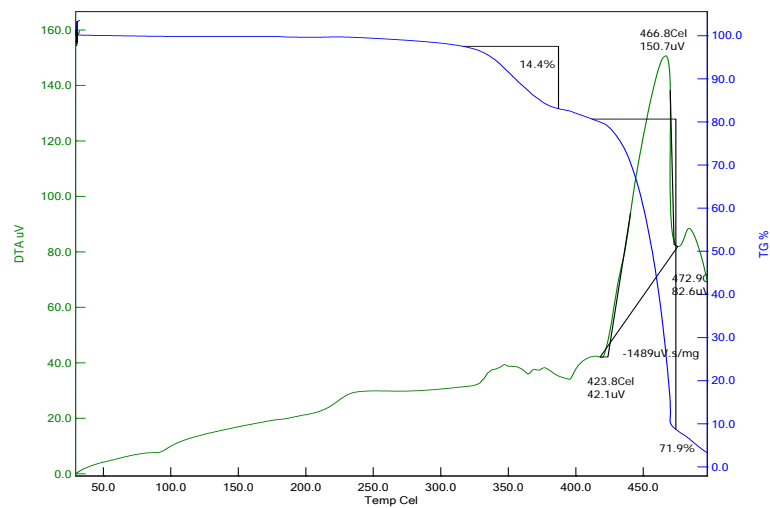
**Figure 11.** (a)-(c) The comparison of FT-IR Spectra of pure EVA, 2%ZnO/EVA and 4%ZnO/EVA polymer nanocomposites.



(a)



(b)



(c)

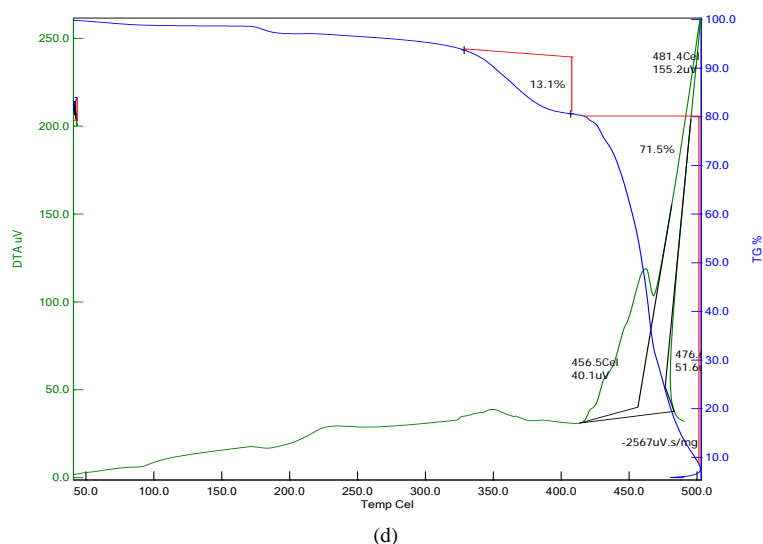


**Figure 12.** (a) TGA-DTA Curve of pure EVA; (b) TGA-DTA Curve of EVA-ZnO 1%; (c) TGA-DTA Curve of EVA-ZnO 2%; (d) TGA-DTA Curve of EVA-ZnO 4%.

medium were thermally thick during measurements. The values of the thermal parameters such as thermal effusivity ( $e$ ) and thermal diffusivity ( $\alpha$ ), the thermal conductivity ( $k$ ) and heat capacity for 2% ZnO are  $1637 \pm 18 \text{ W s}^{1/2}/\text{m}^2\text{K}$ ,  $2.4154 \pm 0.14 \times 10^{-6} \text{ m}^2/\text{s}$ ,  $2.63 \pm 0.10 \text{ W/mK}$  and  $1431 \pm 33 \text{ J/kgK}$  respectively while that of 4% are  $2758 \pm 35 \text{ W s}^{1/2}/\text{m}^2\text{K}$ ,  $8.5113 \pm 0.18 \times 10^{-6} \text{ m}^2/\text{s}$ ,  $7.98 \pm 0.15 \text{ W/mK}$  and  $1300 \pm 28 \text{ J/kgK}$  respectively. When we doubled the filler concentration the value of thermal parameters has got enhanced whereas the specific heat capacity decreased.

### 3.4. Mechanical Properties

The tensile strength and elongation at break of the virgin EVA and EVA nanocomposites samples were performed using an Instron 3366 testing machine according to ASTM D882. Each sample had a width of 6.4 mm. The average thickness of the samples was about 0.060 mm. The tensile test was conducted using a cross head speed of 1.3 mm/min. The stress-strain graph and elongation at various stages of the test was recorded and shown in **Figure 13**. Ethylene vinyl acetate (EVA) films shows good tensile strength (30 MPa) and stretches 430% to its original dimension before break. Thin films of EVA-ZnO nanocomposites have got comparable tensile and deforming properties to that of the virgin polymer. The tensile strength improves to 33 MPa on addition of 1% of ZnO nanoparticles. The nano sized particles tend to tie up the EVA molecules, leading to greater resistance to the tensile deformations. Further increase in ZnO, reduces the tensile strength and the strain deformations. The chain flexibility of the macromolecules might have been reduced with the incorporation of ZnO nanoparticles, leading to reduction of elongation.

Peel strength of the nanocomposites were performed using an Instron tensile testing machine at a peel speed of 50 mm/min. Peel test with  $180^\circ$  stripping is carried out as per ASTM D 1876. Peel test involves stripping away of substrate joined by the adhesive. The substrates (glass paper, cotton and polyester) were flexible enough to permit a  $180^\circ$  turn near the point of loading. Peel strength values was recorded in Newton per millimeter (N/mm) of width of the bonded specimen. Peel strength of the EVA nanocomposites on various substrates are shown in **Figure 14**. The inclusion of the ZnO nanoparticles to the EVA matrix improves its peel strength on 2% of nano ZnO loading on all substrates. When ZnO is added more, it is found that the peel adhesion properties get reduced compared to the virgin compound. The surface finish and smoothness of the glass paper might have attributed to its inferior adhesion compared cotton and polyester fabric. Cotton fabric gives maximum peel adhesion (2.4 N/mm) as the EVA copolymer impregnate on its porous surface.

## 4. Conclusion

The EVA/ZnO nanocomposites materials of different concentrations of ZnO nanoparticle (0%, 1%, 2% and 4%)

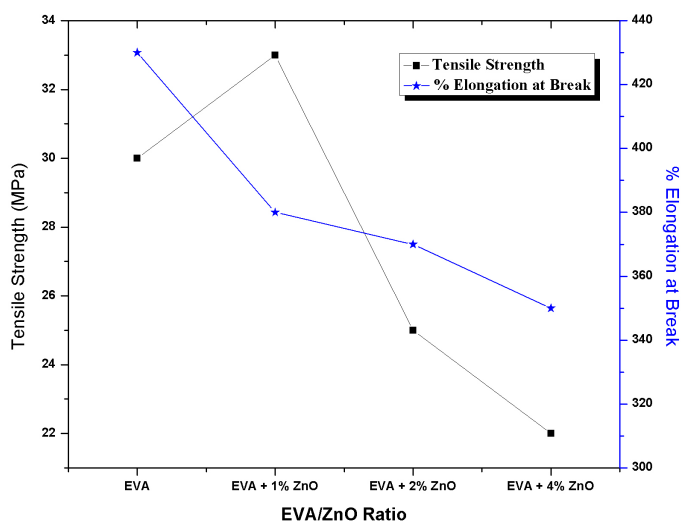


**Figure 13.** Tensile strength and Elongation at break of EVA/ZnO nanocomposite.

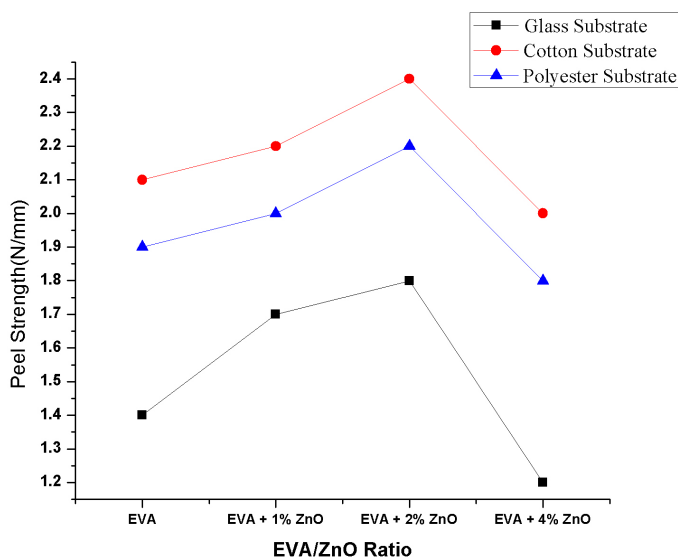


**Figure 14.** Peel strength of EVA/ZnO nanocomposite.

have been prepared successfully by ultrasonic probe method. The ZnO nanoparticles used in the synthesis of polymer nanocomposite were synthesized using solvothermal method. The investigations on the electrical properties of the nanocomposites revealed that the conductivity increases with increasing the filler concentrations and resistivity increases with increasing the temperature. The band gap of the nanocomposites found to be decreased with increasing the filler concentration. The thermal stability of the nanocomposites was also found to be increased. Photopyroelectric Technique is used to find the thermal parameters such as thermal diffusivity ( $\alpha$ ) and thermal effusivity ( $e$ ), the thermal conductivity ( $k$ ) and heat capacity ( $C_p$ ) and except heat capacity all others found to be increased with increasing the filler concentrations. The tensile strength and peel strength of the nanocomposites found to increase initially with the addition of ZnO nanomaterials. On further addition of ZnO, the mechanical properties drop down.

## References

- [1] Ray, S., Easteal, A.J., Cooney, R.P. and Edmonds, N.R. (2009) Structure and Properties of Melt-Processed PVDF/PMMA/Polyaniline Blends. *Materials Chemistry and Physics*, **113**, 829-838.

- <http://dx.doi.org/10.1016/j.matchemphys.2008.08.034>
- [2] Blom, P.W.M., Schoo, H.F.M. and Matters, M. (1998) Electrical Characterization of Electroluminescent Polymer/Nanoparticle Composite Devices. *Applied Physics Letters*, **73**, 3914. <http://dx.doi.org/10.1063/1.122934>
- [3] Kiesow, A., Morris, J.E., Radehaus, C. and Heilmann, A. (2003) Switching Behavior of Plasma Polymer Films Containing silver Nanoparticles. *Journal of Applied Physics*, **94**, 6988. <http://dx.doi.org/10.1063/1.1622990>
- [4] Siegel, R.W., Schadler-Feist, L., Ma, D., Hong, J.I., Martensson, E. and Onneby, C. (2005) Nanocomposites with controlled Electrical Properties. Publication No: WO2005036563, 28 p.
- [5] Murugaraj, P., Mainwaring, D. and Mora-Huertas, N. (2005) Dielectric Enhancement in Polymer-Nanoparticle Composites through Interphase Polarizability. *Journal of Applied Physics*, **98**, 054304. <http://dx.doi.org/10.1063/1.2034654>
- [6] Tishkova, V., Raynal, P.-I., Puech, P., Lonjon, A., Le Fournier, M., Demont, P., Flahaut, E. and Basca, W. (2011) Electrical Conductivity and Raman Imaging of Double Wall Carbon Nanotubes in a Polymer Matrix. *Composites Science and Technology*, **71**, 1326-1330. <http://dx.doi.org/10.1016/j.compscitech.2011.05.001>
- [7] Lee, J., Sunder, V.C., Heine, J.R., Bawendi, M.G. and Jensen, K.F. (2000) Full Color Emission from II-VI Semiconductor Quantum Dot-Polymer Composites. *Advanced Materials*, **12**, 1102. [http://dx.doi.org/10.1002/1521-4095\(200008\)12:15<1102::AID-ADMA1102>3.0.CO;2-J](http://dx.doi.org/10.1002/1521-4095(200008)12:15<1102::AID-ADMA1102>3.0.CO;2-J)
- [8] Shaheen, S.E., Brabec, C.J., Sariciftci, N., *et al.* (2001) 2.5% Efficient Organic Plastic Solar Cells. *Applied Physics Letters*, **78**, 841-843. <http://dx.doi.org/10.1063/1.1345834>
- [9] Wang, H. and Branton, D. (2001) Nanopores with a Spark for Single-Molecule Detection. *Nature Biotechnology*, **19**, 622-623. <http://dx.doi.org/10.1038/90216>
- [10] Artemyev, M., Woggon, U. and Langbein, W. (2002) Quantum Dot Emission Confined by a Spherical Photonic Dot. *Physica Status Solidi (b)*, **229**, 423-426. [http://dx.doi.org/10.1002/1521-3951\(200201\)229:1<423::AID-PSSB423>3.0.CO;2-#](http://dx.doi.org/10.1002/1521-3951(200201)229:1<423::AID-PSSB423>3.0.CO;2-#)
- [11] Klein, D., Roth, R., Lim, A.K.L., Alivisatos, A.P. and McEuen, P.L. (1997) A Single-Electron Transistor Made from a Cadmium Selenide Nanocrystal. *Nature*, **389**, 699-701. <http://dx.doi.org/10.1038/39535>
- [12] Klimov, V.I., Milkhailovsky, A.A., Xu, S. Leatherdale, C.A., Eisler, H.J. and Bawendi, M.G. (2000) Optical Gain and Stimulated Emission in Nanocrystal Quantum Dots. *Science*, **290**, 314-317. <http://dx.doi.org/10.1126/science.290.5490.314>
- [13] Konenkamp, R., Word, R. and Schlegel, C. (2004) Vertical Nanowire Light-Emitting Diode. *Applied Physics Letters*, **85**, 6004. <http://dx.doi.org/10.1063/1.1836873>
- [14] Dang, Z.M., Zhou, T., Yao, S.H., Yuan, J.K., Zha, J.W. and Song, H.T. (2009) Advanced Calcium Copper Titanate/Polyimide Functional Hybrid Films with High Dielectric Permittivity. *Advanced Materials*, **21**, 2077-2082. <http://dx.doi.org/10.1002/adma.200803427>
- [15] Dang, Z.M., Yuan, J.K., Zha, J.W., Zhou, T., Li, S.T. and Hu, G.H. (2012) Fundamentals, Processes and Applications of High-Permittivity Polymer-Matrix Composites. *Progress in Materials Science*, **57**, 660-723. <http://dx.doi.org/10.1016/j.pmatsci.2011.08.001>
- [16] Monti, O.L.A., Fourkas, J.T. and Nesbitt, D.J. (2004) Diffraction-Limited Photogeneration and Characterization of Silver Nanoparticles. *The Journal of Physical Chemistry B*, **108**, 1604-1612. <http://dx.doi.org/10.1021/jp030492c>
- [17] Yuen, S.M., Ma, C.C.M., Chuang, C.Y., Yu, K.C., Wu, S.Y., Yang, C.C. and Wei, M.H. (2008) Effect of Processing Method on the Shielding Effectiveness of Electromagnetic Interference of MWCNT/PMMA Composites. *Composites Science and Technology*, **68**, 963-968. <http://dx.doi.org/10.1016/j.compscitech.2007.08.004>
- [18] Stankovich, S., Dikin, D.A., Dommett, G.H.B., Kohlhaas, K.M., Zimney, E.J., Stach, E.A., Piner, R.D., Nguyen, S.T. and Ruoff, R.S. (2006) Graphene-Based Composite Materials. *Nature*, **442**, 282-286. <http://dx.doi.org/10.1038/nature04969>
- [19] Khanna, P.K., Singh, N., Charan, S. and Mulik, U.P. (2005) Synthesis and Characterization of Ag/PVA Nanocomposite by Chemical Reduction Method. *Materials Chemistry and Physics*, **93**, 117-121.
- [20] Bhadra, S., Khastgir, D., Singha, N.K. and Lee, J.H. (2009) Progress in Preparation, Processing and Applications of Polyaniline. *Progress in Polymer Science*, **34**, 783-810. <http://dx.doi.org/10.1016/j.progpolymsci.2009.04.003>
- [21] Subramanian, S. and Pathinettam Padiyan, D. (2008) Effect of Structural, Electrical and Optical Properties of Electrodeposited Bismuth Selenide Thin Films in Polyaniline Aqueous Medium. *Materials Chemistry and Physics*, **107**, 392-398. <http://dx.doi.org/10.1016/j.matchemphys.2007.08.005>
- [22] Gonzalez-Benito, J., Castillo, E. and Caldito, J.F. (2013) Coefficient of Thermal Expansion of TiO<sub>2</sub> Filled EVA Based Nanocomposites. A New Insight about the Influence of Filler Particle Size in Composites. *European Polymer Journal*, **49**, 1747-1752. <http://dx.doi.org/10.1016/j.eurpolymj.2013.04.023>

- [23] Chu, K.C., Jordan, K.J., Battista, J.J., Van-Dyk, J. and Rutt, B.K. (2000) Polyvinyl Alcohol-Fricke Hydrogel and Cryogel: Two New Gel Dosimetry Systems with Low  $\text{Fe}^{3+}$  Diffusion. *Physics in Medicine and Biology*, **45**, 955.  
<http://dx.doi.org/10.1088/0031-9155/45/4/311>
- [24] Kasap, S. (2007) Springer Handbook of Electronic and Photonic Materials. Springer, Berlin.  
<http://dx.doi.org/10.1007/978-0-387-29185-7>
- [25] Preethy Menon, C. and Philip, S. (2000) Simultaneous Determination of Thermal Conductivity and Heat Capacity Near Solid State Phase Transitions by a Photopyroelectric Technique. *Measurement Science and Technology*, **11**, 1744.  
<http://dx.doi.org/10.1088/0957-0233/11/12/314>